Self-Resonant Structures of Normal-Mode Helical Antennas embedded in Dielectric and Magnetic Materials

Nguyen Thanh Tuan, Yoshihide Yamada
Malaysia-Japan International Institute of Technology, Universiti Teknologi Malaysia
Kuala Lumpur, Malaysia
nguyentuan.dt9@gmail.com,
ndayamada@yahoo.co.jp

Nguyen Quoc Dinh
Department of Fundamentals of Radio and Electronics Engineering
Le Quy Don Technical University
Hanoi, Vietnam
dinhnq@mta.edu.vn

Naobumi Michishita
Department of Electric and Electronics Engineering
National Defense Academy
Yokosuka Japan
naobumi@nda.ac.jp

***Abstract*— Normal-mode helical antennas (NMHA) are well known for achieving high antenna efficiencies in very small sizes when antenna structures are tuned to self-resonant situations. The design equation determining self-resonant structures were developed in free space conditions. However, in practically, NMHA mostly used dielectric or magnetic materials as cores. The design equation for these cases is not studied yet.**

In this paper, fundamental self-resonant structures are studied for NMHA placed in dielectric or magnetic material. In order to obtain correct calculation results, calculation models of an commercial electromagnetic simulator (FEKO) is studied. Many data for structural change from free space condition to inside materials are achieved. Moreover, input resistance and antenna efficiency changes are also obtained.

Keywords*— *Normal-mode Helical Antenna, Self-resonant Structure, dielectric material, magnetic material.

I. INTRODUCTION

Normal-mode helical antennas are very attractive because of achieving rather high antenna efficiencies at 1/100 wavelength size [1]. In order to make the antenna works efficiently, antenna structures should be designed at self-resonant situations. Authors developed a design equation for self-resonant structures based on electric and magnetic fields calculated by electromagnetic simulator and theoretical analysis on antenna input capacitances [2]. Some application possibilities are considered for Radio Frequency Identification (RFID) tag antennas [3] and Tire-Pressure Monitoring System (TPMS) inside car tire [4]. As for another applications, very small medical sensors for human body are promising [5][6]. Here, NMHA is placed in a human tissue and antenna self-resonant structure may be differ from the free space. Previously, authors obtained self-resonant structure data for dielectric or magnetic materials are inside NMHA [7]. For the case of NMHA embedded in a material, new structural study should be necessary.

In this paper, firstly, a suitable simulation model to achieve correct calculation results is investigated at frequency of 900 MHz. At the same time, the adequate dielectric size is also determined. Self-resonant structures for dielectric and magnetic materials are studied. In both cases, reductions of NMHA diameters are obtained for increasing dielectric or magnetic constants. Moreover, electric and magnetic fields changes, input resistance changes and antenna efficiency changes are also obtained. Through this study, almost fundamental characteristics of material loadings are clarified.

II. SELF-RESONANT STRUCTURES IN FREE SPACE

A configuration of NMHA is shown in Fig. 1. H_A, D_A, N are length, diameter and number of turns of antenna, respectively. The diameter of the antenna wire is noted by d. An equivalent current model is shown in Fig. 1(b). A spiral current is divided to a strait current and a loop current. The strait current corresponds to a small dipole antenna and has an input impedance of R_{rD} - jX_D. Here, X_D is a capacitive reactance. The loop current corresponds to small loop antenna and has an input impedance of R_{rL} + jX_L. Here, X_L is an inductive reactance. A self-resonant condition of a NMHA is given by $X_D = X_L$.

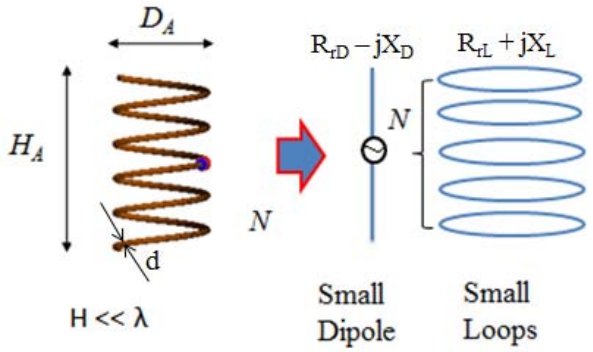

(a) Antenna parameters (b) Equivalent current model

Fig. 1 Configuration of normal-mode helical antenna

When $X_D = X_L$ is expressed by using antenna parameters, the next equation is given [2].

$$\frac{279\frac{H_A}{\lambda}}{N\pi(0.92\frac{H_A}{\lambda}+\frac{D_A}{\lambda})^2} = \frac{600\pi\times 19.7N(\frac{D_A}{\lambda})^2}{9\frac{D_A}{\lambda}+20\frac{H_A}{\lambda}} \quad (1)$$

This equation determines self-resonant structures of NMHA. Comparisons of structures obtained by Eq. (1) and by electromagnetic simulator are shown in Fig. 2. From the good agreement of equation results to simulation results, the usefulness of Eq. (1) is ensured. Besides, electromagnetic simulation conditions are shown in Table. 1. The employed simulator is FEKO suite 7.0 [8]. In calculation, the antenna wire is divided into very small segments whose length is 1/300 wave length at the calculation frequency of 900 MHz. Diameter of antenna wire is selected by d = 0.5 mm. Conductivity of antenna wire (σ) is set to 58 x 10^6 [1/Ωm] of a copper. In simulation, self-resonant structures are determined by watching a Smith chart results for changing antenna structures.

Electric and magnetic fields at the self-resonant structure shown by A in Fig.2 are shown in Fig. 3. As a unique point of electric field distribution, diverging and converging areas are observed at the opposite sides of the antenna. These areas are considered positive charge and negative charge areas. Using these areas, antenna capacitive reactance (X_D) expression of Eq. (1) is deduced.

Antenna input impedance is expressed by the next equation:

$$Z_{in} = R_{rD} + R_{rL} + R_l + j(X_L - X_D) \quad (2)$$

Here, R_{rD} is the radiation resistance of the small dipole; R_{rL}, the radiation resistance of the small loops; and R_l is the ohmic resistance of the antenna wire. X_L and X_D are the inductive and capacitive reactance, respectively. The expressions for resistances are given by following equations.

$$R_{rD} = 20\pi^2 \left(\frac{H}{\lambda}\right)^2 \quad (3)$$

$$R_{rL} = 320\pi^6 \left(\frac{D}{2\lambda}\right)^4 N^2 \quad (4)$$

$$R_l = \alpha \frac{L}{d}\sqrt{\frac{120}{\lambda\sigma}} \quad (5)$$

In Eq. (5), α is the coefficient of tapered current distribution, α= 0.6. L is the total length of the wire and σ is conductivity of the wire. Important characteristics of resistances are as follows. R_{rD} becomes proportional to the antenna length (H/λ). R_{rL} is proportional to antenna diameter (D/λ) and antenna turns (N). R_l is proportional to the total length of wire (L) and inversely proportional the diameter of wire (d).

Table. 1 Simulation parameters of NMHA in free space

Simulator	FEKO 7.0 (MoM)
Frequency	900 MHz
d	0.5 mm
Number of turns	N = 5; 7; 10
Mesh size	1/300 wavelength
Metallic wire	Copper (σ = 58 x 10^6 [1/Ωm])

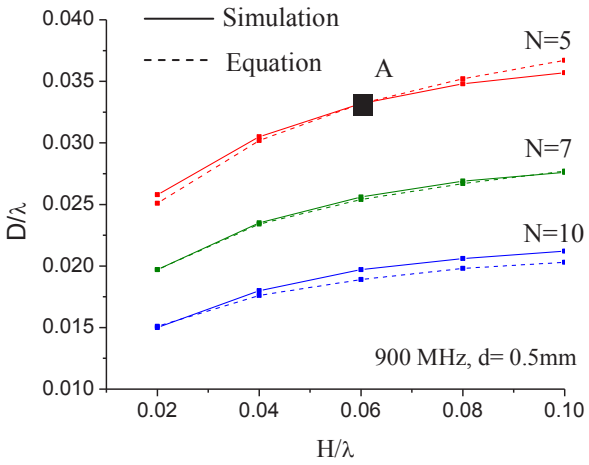

Fig.2 Self-resonant Structures of NMHA in free space

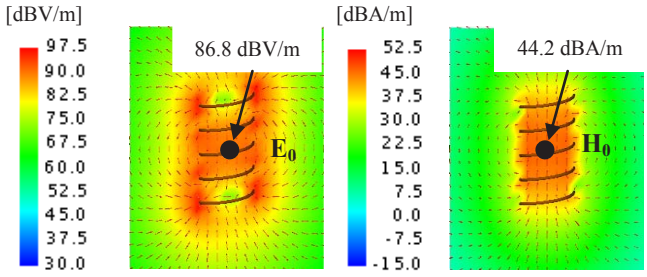

(a) Electric field distributions (b) Magnetic field distributions

Fig.3 Electric and magnetic near field of NMHA in free space

III. SIMULATION CONDITION

A. Simulation model

In order to make simulation the structure that NMHA is embedded in a large material. Simulation models are studied on FEKO MoM scheme. In MoM calculation, antenna wire and material are divided into small calculation segments. It is considered that at the contact portion of antenna and material, size mismatch of segments may exist. This mismatch may cause some calculation errors. So, the structure shown in Fig. 4 is selected. Between antenna wire and material, a narrow space is placed. As for the volume of material, by taking into account electric and magnetic field expansion outside NMHA shown in Fig. 3, material sizes of outside NMHA is set 30 mm. Simulation parameters of materials are shown in Table. 2. Dielectric and magnetic materials are studied. For calculating these materials, SEP (Surface Equivalent Principle) model is employed. Mesh sizes of materials are set to be 1/30 wavelength to meet the accuracy of calculation and computing capabilities of a personal computer. Relative permittivity (ε_r) and relative permeability (μ_r) of 1, 5 and 10 are considered. Calculation time is about 36 minutes for one self-resonant curve.

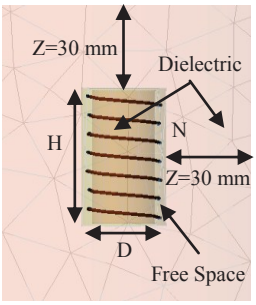

Fig. 4 Simulation model

Table. 2 Simulation parameters of NMHA in materials

Simulator	FEKO 7.0 (MoM)
Frequency	900 MHz
d	0.5 mm
Number of turns	N = 5; 7; 10
Mesh size	Antenna: 1/300 wavelength Dielectric(Magnetic): 1/30 wavelength
Metallic wire	Copper ($\sigma = 58 \times 10^6$ [1/Ωm])
Dielectric Material	ε_r= 1; 5; 10
Magnetic Material	μ_r= 1; 5; 10
Calculation time	36 minutes/ one resonant curve

B. *Simulation accuracies*

At first, adequate mesh sizes of materials are investigated. Calculated results of electromagnetic near fields and input impedance locus are shown in Fig. 5. Electromagnetic fields in materials become almost same for different mesh sizes of λ/10, λ/20 and λ/30. However, in input impedance data, 900 MHz points are moving slightly. At λ/30 mesh size, 900 MHz point seems converged. As a result, mesh size of λ/30 is selected for calculation.

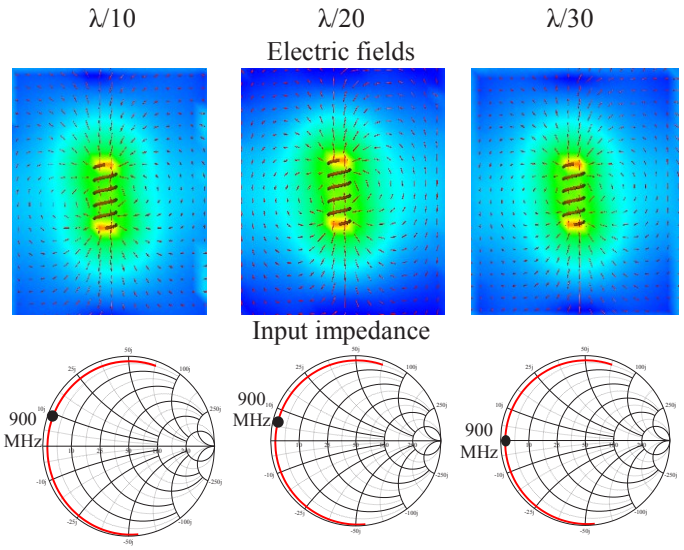

(a) Dielectric

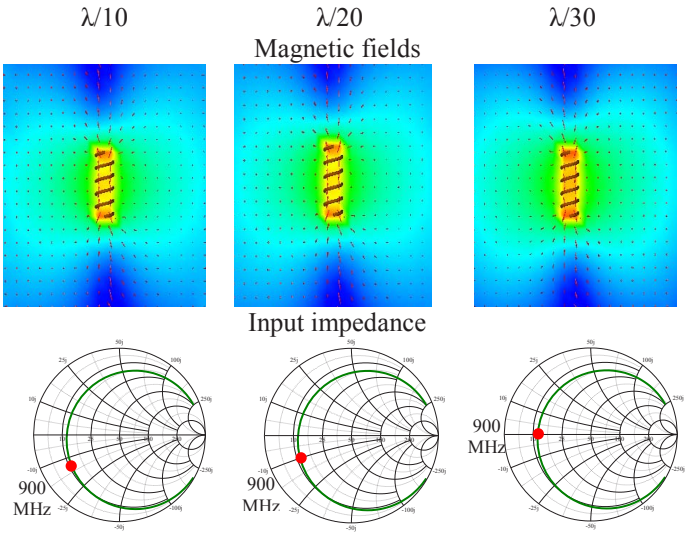

(b) Magnetic

Fig. 5 Convergence of calculated results

IV. SIMULATED RESULTS

A. *NMHA in dielectric materials*

1) *Electric and magnetic near field*

Field distributions at the structure C of Fig. 7 are shown in Fig. 6. Here, ε_r= 10 is used. By comparing the results of Fig. 6 with that of Fig. 3, although magnetic fields seem unchanged, electric field is decreased almost 10 dB. The reduction value agrees very well with the dielectric constant increase of 10 times. The reduction of electric field in a dielectric material reminds the effect of electric polarization.

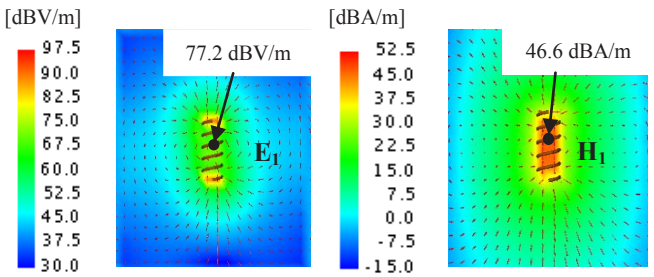

(a) Electric field distributions

(b) Magnetic field distributions

Fig. 6 Electric and magnetic near field distributions of NMHA in dielectric material

2) *Self resonant structures*

Calculated self-resonant structures in dielectric materials are shown in Fig. 7 to 9. Antenna structure changes compared to free space case are shown for different N values. Antenna diameters (D/λ) are decreased in increasing dielectric

constants (ε_r). In order to understand well the diameter decrease, diameter reduction ratio ($\gamma = D_i / D_1$) is considered. Here, D_1 is the diameter of $\varepsilon_r = 1$. D_i indicates the diameter of dielectric material loading. Results of γ are shown in Fig. 10. As an interesting result, γ is not affected by N changes. γ is only dependent to ε_r changes. γ reduces in increasing ε_r values.

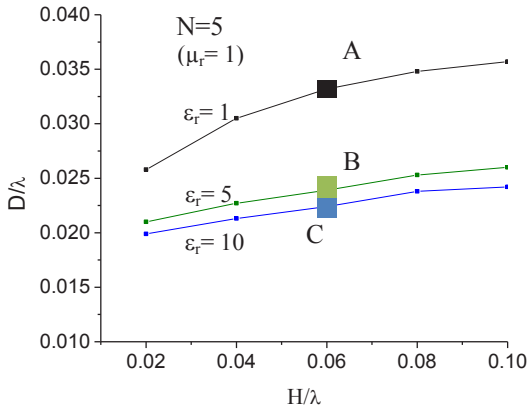

Fig. 7 Self-resonant structures with dielectric of N= 5

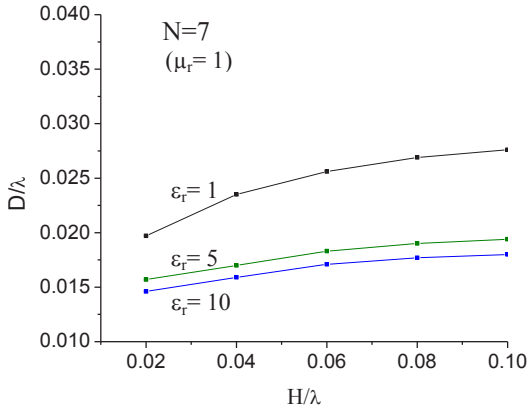

Fig. 8 Self-resonant structures with dielectric of N= 7

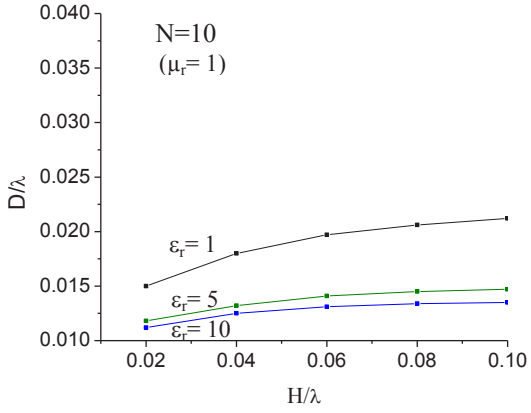

Fig. 9 Self-resonant structures with dielectric of N= 10

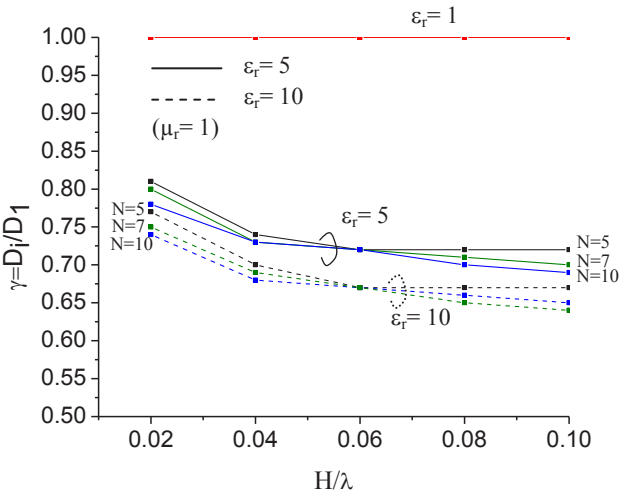

Fig. 10 The changes of antenna diameters

3) Input resistances and Antenna efficiency

Antenna input resistances are estimated by Eq. (3), Eq. (4) and Eq. (5). Calculated results of R_{in} and R_l by an electromagnetic simulator are shown in Fig. 11. In the case of R_{in}, values seem to depend on only H/λ and not affected by ε_r changes. However, R_l value seem to depend on ε_r changes. This is because of decrease of total wire length (L) in accordance with the diameter (D/λ) decreases in ε_r increases. By using values of R_{in} and R_l, antenna efficiency is expressed as follows:

$$\eta = 1 - \frac{R_l}{R_{in}} \tag{6}$$

Calculated results by an electromagnetic simulator are shown in Fig. 12. It is observed that η is not affected by ε_r changes.

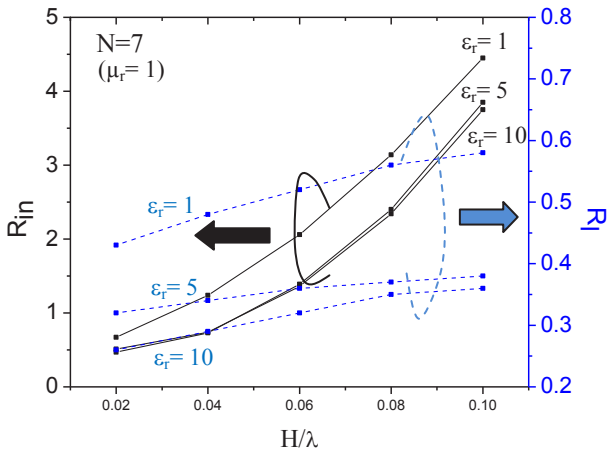

Fig. 11 Input resistances and ohmic resistances of NMHA in dielectric material

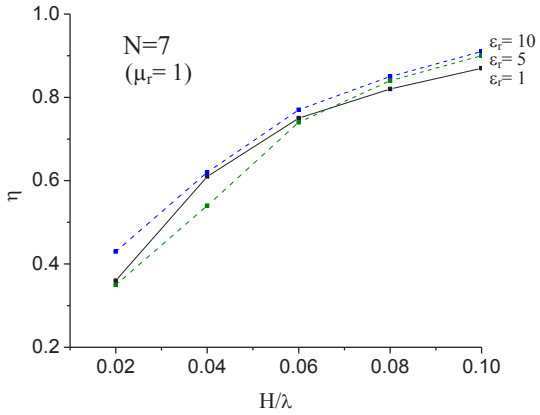

Fig. 12 Antenna efficiencies of NMHA in dielectric material

B. NMHA in magnetic materials

1) Electric and magnetic near field

Field distributions at the structure E of Fig. 14 are shown in Fig. 13. Here, $\mu_r = 10$ is used. By comparing the results of Fig. 13 with that of Fig. 3, although electric fields seem unchanged, magnetic field is decreased almost 10 dB. The reduction value agrees very well with the magnetic constant increase of 10 times. The reduction of magnetic field in a magnetic material reminds the effect of magnetic polarization.

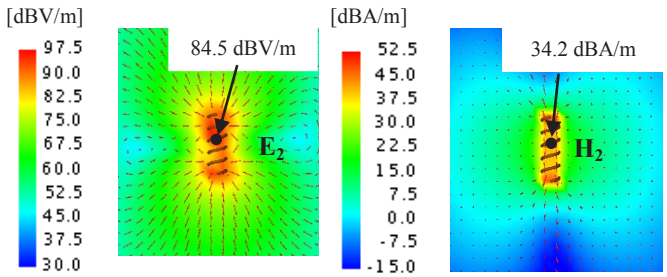

(a) Electric field distributions (b) Magnetic field distributions

Fig. 13 Electric and magnetic near field distributions of NMHA in magnetic material

2) Self resonant structures

In the case of NMHA is embedded in magnetic material, self-resonant structures, electric and magnetic field distributions, input impedances and antenna efficiency are investigated. Calculated self-resonant structures in magnetic materials are shown in Fig. 14 to 16. Antenna structure changes compared to free space case are shown for different N values. Antenna diameters (D/λ) are decreased in increasing magnetic constants (μ_r). Results of diameter reduction ratio γ are shown in Fig. 17. As an interesting result, γ is not affected by N changes, γ is dependent to μ_r changes. γ reduces in increasing μ_r values.

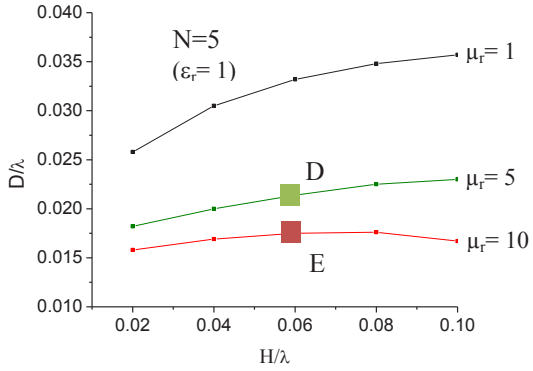

Fig. 14 Self-resonant structures with magnetic of N= 5

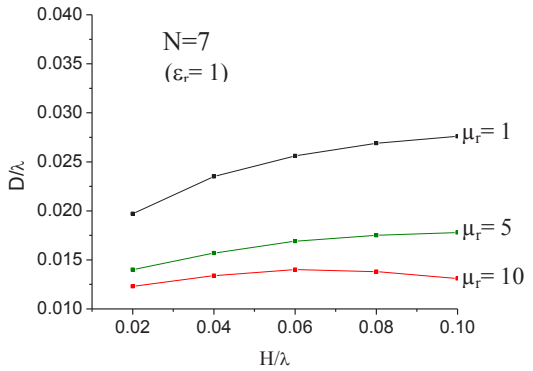

Fig. 15 Self-resonant structures with magnetic of N= 7

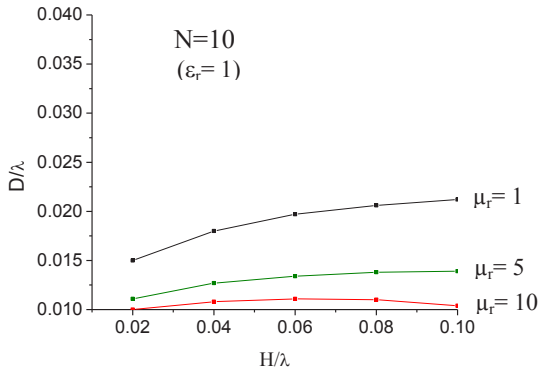

Fig. 16 Self-resonant structures with magnetic of N= 10

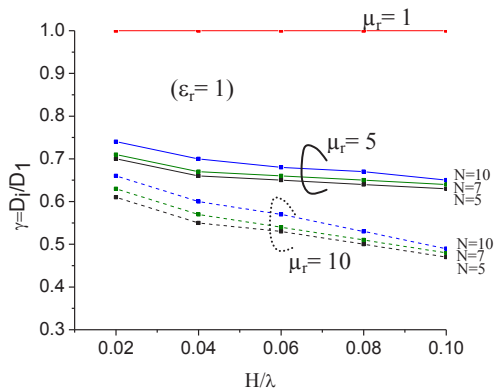

Fig. 17 The changes of antenna diameters in magnetic material

3) Input resistances and Antenna efficiency

In the case of magnetic material, R_{rL} of Eq. (4) is modified to the next expression.

$$R_{rL} = 31200\left(\mu_r \frac{\pi D^2}{4\lambda^2}\right)^2 N^2 \qquad (7)$$

Calculated results by an electromagnetic simulator are shown in Fig. 18. As expected by Eq. (7), R_{in} increases in accordance with the increase of μ_r. R_l is decrease because of decreases of antenna diameter (D/λ) in μ_r increase. R_{in} increase is expected to produce antenna efficiency (η) increase. Simulation results of η are shown in Fig. 19. Remarkable η increases are shown in the figure.

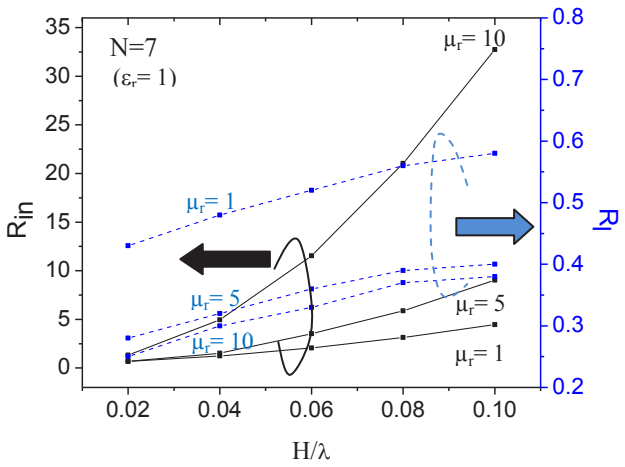

Fig. 18 Input resistances and ohmic resistances of NMHA in magnetic material

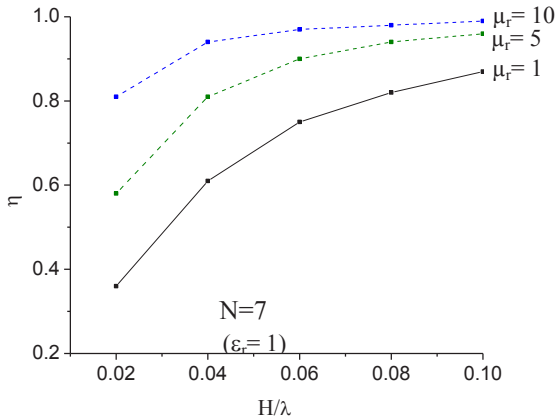

Fig. 19 Antenna efficiency of NMHA in magnetic material

V. CONCLUSION

From calculation results of an electromagnetic simulator (FEKO), following important characteristics are clarified for NMHA embedded in dielectric or magnetic materials.

1. Self-resonant structures are clarified for the case of NMHAs are embedded in dielectric and magnetic structures.
2. Antenna diameters are decreased for increasing material constants.
3. Electric and magnetic fields are decreased for increasing material constants.
4. Antenna input resistance and efficiency are increased for increasing magnetic constants. In the case of μ_r = 10, antenna efficiency more than 80% can be achieved.
5. Dielectric material does not affect antenna input resistance and antenna efficiency.

REFERENCES

[1]. Yoshihide Yamada and Naobumi Michishita, "Design Methods and Electrical Performances of Small Normal-Mode Helical Antennas", IEICE, Trans. Commun. B, Vol. J96-B, No.9, PP.894-906, Sept. 2013

[2]. Quoc Dinh Nguyen, Naobumi Michishita, Yoshihide Yamada and Koji Nakatani, "Deterministic Equation for Self-Resonant Structures of Very Small Normal-Mode Helical Antennas", IEICE Trans.Commun., Vol.E94-B, No.5, PP.1276-1279, May 2011

[3]. Won Gook Hong, Naobumi Michishita and Yoshihide Yamada, "Low-profile Normal-Mode Helical Antenna for Use in Proximity to Metal", ACES Journal, Vol.25, No.3, PP.190-198, March 2010

[4]. Nguyen Quoc Dinh, Takashi Teranishi, Naobumi Michishita, Yoshihide Yamada and Koji Nakatani, "FEKO-Based Method for Electromagnetic Simulation of Carcass Wires Embedded in Vehicle Tires", ACES Journal, Vol.26, No.3, PP.217-224, March 2011

[5]. Toshihiro Kumagai, Kazuyuki Saito, Masaharu Takahashi, Koichi Ito, "A Small 915 MHz Receiving Antenna for Wireless Power Transmission Aimed ar Medical Applications", International Journal of Technology (2011) 1: 20-27, ISSN 2086-9614

[6]. Haiyu Huang, Karl Nieman, Ye Hu and Deji Akinwande, "Electrically Small Folded Ellipsoidal Helix Antenna for Medical Implant Applications", AP-S/URSI 2011 IEEE

[7]. K. Ochiyama, N. Michishita and Y. Yamada, "Effects of dielectric or magnetic materials to electrical characteristics of very small nornal-mode helical antennas" Antennas Propag. Soc. Int. Symp., pp. 1-2, Jul. 2012.

[8]. FEKO suite 7, EM Software & Systems